J Solid State Electrochem (2010) 14:1117–1124
DOI 10.1007/s10008-009-0927-x

ORIGINAL PAPER

Low temperature synthesis of $LiNiO_2$@$LiCoO_2$ as cathode materials for lithium ion batteries

Xian-Zhu Fu · Xin Wang · Hong-Feng Peng · Fu-Sheng Ke · Jun-Hu Lei · Ling Huang · Jing-Dong Lin · Dai-Wei Liao

Received: 25 March 2009 / Revised: 6 August 2009 / Accepted: 19 August 2009 / Published online: 29 August 2009

Abstract Spherical $LiNiO_2$@$LiCoO_2$ as cathode material for lithium ion batteries was synthesized by firing the mixture of β-NiOOH@β-CoOOH and LiOH at low temperature in air atmosphere. The effect of synthesis conditions on the structure of the resultant samples was investigated by X-ray diffraction, scanning electron microscope, and energy dispersive spectroscope. Spherical $LiNiO_2$@$LiCoO_2$ obtained at 600 °C for 24 h exhibited best layered hexagonal structure and remained core-shell property. Electrochemical test demonstrated that $LiNiO_2$@$LiCoO_2$ had high initial discharge capacity of 181.4 mA h g^{-1}, better cycle, and storage stability than pure $LiNiO_2$ prepared from spherical β-NiOOH.

Keywords $LiNiO_2$@$LiCoO_2$ · NiOOH@CoOOH · Low temperature synthesis · Lithium ion batteries

X.-Z. Fu (✉) · F.-S. Ke · J.-H. Lei · L. Huang · J.-D. Lin · D.-W. Liao (✉)
State Key Laboratory of Physical Chemistry on Solid Surfaces, Department of Chemistry, College of Chemistry and Chemical Engineering, Institute of Physical Chemistry, Xiamen University, Xiamen 361005, People's Republic of China
e-mail: xzfu@xmu.edu.cn
e-mail: dwliao@xmu.edu.cn

X. Wang
Department of Physics, School of Physics and Mechanical & Electrical Engineering, Xiamen University, Xiamen, Fujian 361005, China

H.-F. Peng
Gold Sky Energy Materials Co., Ltd., Xiangtan 411132, People's Republic of China

Introduction

$LiNiO_2$ is one of the most promising cathode materials for lithium ion batteries due to its lower cost and higher capacity in comparison with $LiCoO_2$ which has been widely utilized in the commercial lithium ion batteries [1, 2]. However, some problems of $LiNiO_2$, such as difficult preparation, instability during the charge–discharge cycle, and storage, need to be solved for its commercialization [3].

The traditional synthesis of $LiNiO_2$ is usually use of bivalent nickel salt and lithium salt at high temperature in oxygen atmosphere due to the difficulty of oxidizing bivalent nickel to form layer-structured $LiNiO_2$ [4]. However, stoichiometric $LiNiO_2$ with good electrochemical property is hard to obtain and unstable at high temperature [5]. Furthermore, it is not convenient to produce $LiNiO_2$ in large scale if oxygen gas is necessary during the preparation process. Recently, $LiNiO_2$ with excellent layered structure was successfully prepared at low temperature even in air atmosphere when trivalent nickel oxide NiOOH was used as precursor [6–8].

To improve the electrochemical performance and stability of $LiNiO_2$, both doping and coating have been intensively investigated. Among the dopants, Co is almost the best one to prepare $LiNi_{1-x}Co_xO_2$ with attractive performance [9–11]. On the other hand, electrochemical active coating is very attractive. $LiNi_{0.5}Mn_{0.5}O_2$ was reported as coating covered on the spherical $Li(Ni_{0.8}Co_{0.1}Mn_{0.1})O_2$ and $LiNi_{0.8}Co_{0.2}O_2$, resulting in a core-shell structure with outstanding electrochemical performance and thermal stability [12–14]. Co-coated $LiNiO_2$ was prepared by $Ni(OH)_2$ coated with $Co(OH)_2$ as precursor,

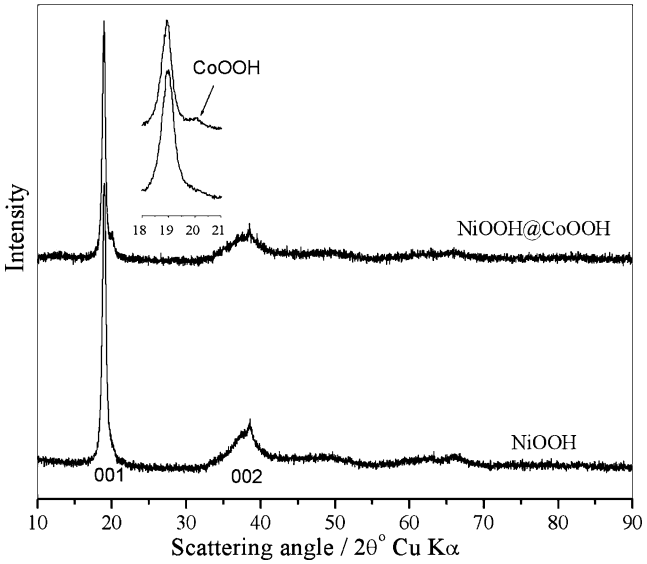

Fig. 1 XRD patterns of NiOOH@CoOOH and NiOOH

which showed better electrochemical properties than $LiNiO_2$ and Co-doping $LiNiO_2$ [15].

Here, we prepared $LiNiO_2$@$LiCoO_2$ from spherical NiOOH@CoOOH precursor at low temperature in air combing the advantages of NiOOH as precursor and core-shell structure with active Co coating modification. The preparation conditions were optimized, the electrochemical and storage performance of $LiNiO_2$@$LiCoO_2$ were also investigated.

Experimental

Spherical NiOOH@CoOOH was prepared similar to our previous work [16] by adding $CoSO_4$ solution containing commercial spherical β-$Ni(OH)_2$ powders into 1 M KOH and ammonia solution at 60 °C (the molar ratio of Ni and Co was 85:15), followed by adding excess amount of $K_2S_2O_8$. After reaction, the black product was washed and dried at 60 °C. For comparison, spherical NiOOH was prepared by adding only spherical β-$Ni(OH)_2$ powders and excess amount of $K_2S_2O_8$ into 1 M KOH solution at 60 °C without $CoSO_4$. The mixture of NiOOH@CoOOH and LiOH salt with a molar ratio of $Li/(Ni + Co) = 1.05$ was heated at different temperatures and times in air in order to optimize the synthetic condition of $LiNiO_2$@$LiCoO_2$.

The phase structure of samples was identified by X-ray diffraction (XRD) measurements. It was carried out on a X'Pert PRO X-ray Diffractometer ($Cu\,K_\alpha$ radiation, λ= 1.540598 Å) with scan step of 0.008° (2θ) for 5 s at 40 kV and 30 mA. Morphology and metal content of samples were observed using a LEO1530 Field Emission Scanning Electron Microscope (SEM) with Oxford Instrument energy dispersive spectroscope (EDS). The total oxidation state of Ni and Co in the products was analyzed by iodometry and EDTA titration. Typically, 100 mg of the product was mixed with 2 g of KI and added into 0.5 M H_2SO_4 solution. The solution was then placed in the dark for 1 h, and the I_2 produced from the nickel and cobalt reduction was titrated with 0.1 M $Na_2S_2O_3$ using starch as an indicator. 10% NH_3 solution was added to neutralize the

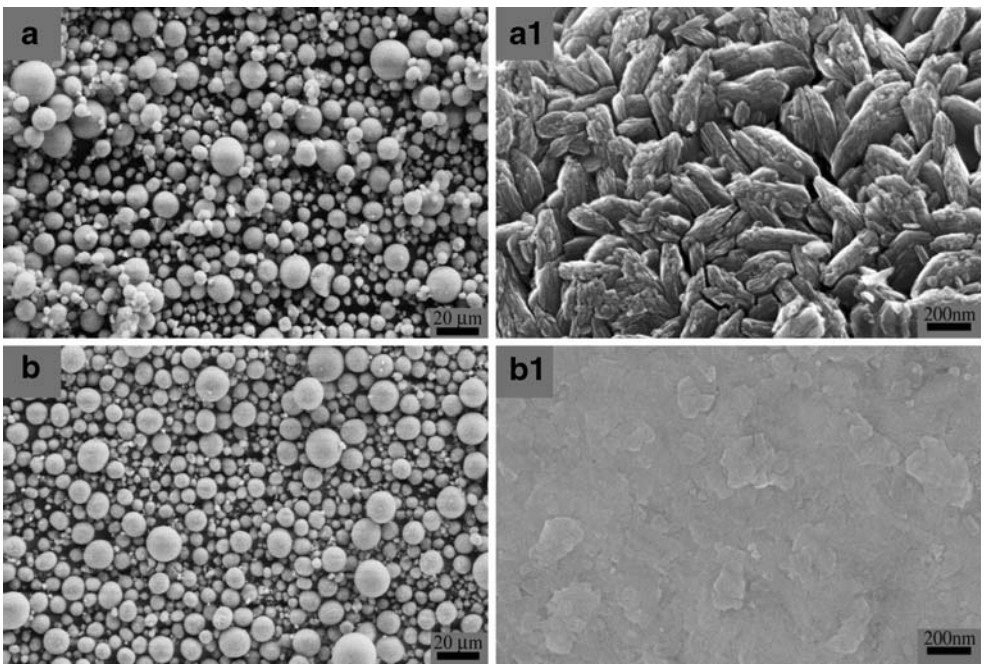

Fig. 2 SEM images of β-NiOOH(*a* and *a1*) and β-NiOOH@β-CoOOH(*b* and *b1*)

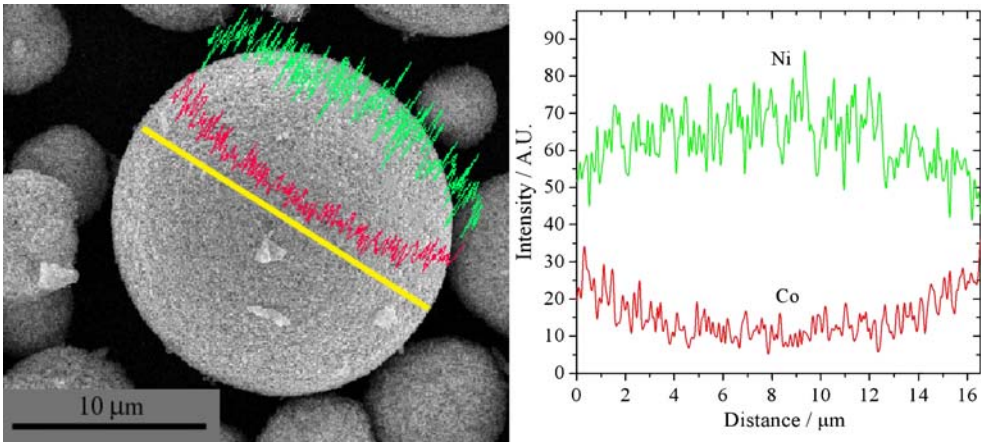

Fig. 3 EDS image of β-NiOOH@β-CoOOH particle

excess acid, and NH_4Cl/NH_3 buffer solution was added (pH=10) as well. The total amount of nickel and cobalt was titrated with 0.1 M EDTA using murexide as an indicator.

The electrochemical performance of the samples was measured using CR2025 coin cells. The cathode was prepared by mixing 85% of $LiNiO_2$@$LiCoO_2$ or $LiNiO_2$ with 10% carbon black and 5% polyvinylidene fluoride. The lithium metal was as anode, and Celgard 2300 film was as separator. The electrolyte consisted of a solution of 1 M $LiPF_6$ in a mixture of ethylene carbonate/dimethyl carbonate/diethyl carbonate (1:1:1; vol%). Charge and discharge experiment was conducted at current density of 20 mA g^{-1} with a BS-9300R battery tester.

The storage stability of samples was evaluated by comparing the weight increment percent of $LiNiO_2$@$LiCoO_2$ and $LiNiO_2$ in 65% humidity at 30 °C. If the sample reacts with H_2O and CO_2 in the atmosphere, its weight will increase so the weight increment can indicate the storage stability.

Results and discussion

Figure 1 shows the XRD pattern of the NiOOH@CoOOH comprising intensive β-NiOOH (JCPDS 6-0141) diffraction peaks and weak β-CoOOH (JCPDS 14-0673) diffraction peak. As known from the synthetic process, it was obvious that β-$Ni(OH)_2$ particles was deposited by $Co(OH)_2$ precipitation when the $CoSO_4$ solution containing spherical β-$Ni(OH)_2$ powders was poured into the alkaline solution, moreover, the amount of $Ni(OH)_2$ was larger than $Co(OH)_2$ according to the fixed Ni/Co ratio. The XRD result suggested that β-$Ni(OH)_2$ and $Co(OH)_2$ were separately oxidized to β-NiOOH and β-CoOOH, respectively.

Figure 2 (a) and (b) illustrate that both β-NiOOH@β-CoOOH and β-NiOOH are similar uniform spherical powders from the low-magnification SEM images. Nevertheless, the high-magnification surface image of β-NiOOH@β-CoOOH in Fig. 2 (a1) is significantly different from that of spherical β-NiOOH powder in Fig. 2 (b1). The pure β-NiOOH surface is made up of smaller granular crystalline grains, whereas, the β-NiOOH@β-CoOOH surface is completely covered by another smoother layer. The result indicates the successful coating on the surface of pristine spherical β-NiOOH particles. The EDS analysis result at the line yellow on the spherical NiOOH@CoOOH particle is shown in Fig. 3. It demonstrates that the Co content decreases while the Ni content increase from the edge to the center (about 8.5 μm distance in the EDS

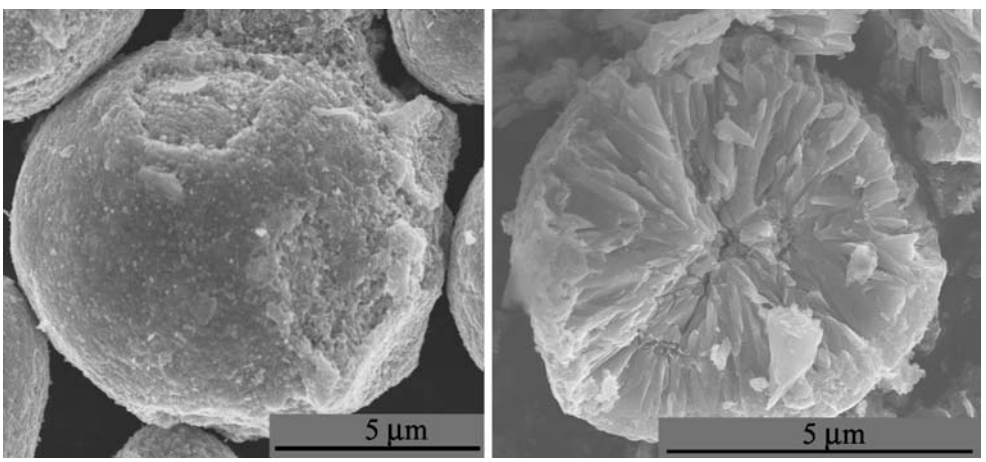

Fig. 4 SEM images of broken β-NiOOH@β-CoOOH particles

image) of the spherical particle, meaning that Co element appears in abundance compared to Ni in the shell (β-CoOOH as shell and β-NiOOH as core). Furthermore, the SEM images of broken particles in Fig. 4 clearly confirm the core-shell structure of NiOOH@CoOOH.

Figure 5 displays the XRD patterns of the samples prepared by sintering the mixture of spherical β-NiOOH@β-CoOOH and LiOH at temperatures of 500, 550, 600, 650, 700, 750, and 800 °C for 24 h, respectively. It can be observed that all the samples have layered hexagonal structure with a space group of R-3m with trace of Li_2CO_3 which might be attributed to the reaction of LiOH and CO_2 in the air [7]. The I_{003}/I_{104} of the samples is summarized in Fig. 6, which can be used to determine the degree of ordering layered property (generally the $I_{003}/I_{104}>1.2$) [6, 7, 17]. The result reveals that the I_{003}/I_{104} increased from 1.54 to 1.79 as the sintering temperature from 500 to 600 °C at first, then decreased to 1.31 when the sintering temperature continued to 700 °C. It means that the sample sintered at 600 °C has the best layered structure, the temperature is lower than that of $Ni(OH)_2$ as precursor [5]. The total oxidation state of Ni and Co is high at about 3. So the layered hexagonal structured $LiNiO_2$-$LiCoO_2$ can be obtained at low temperature in the air atmosphere.

It is seen from SEM images in Fig. 7 that the surfaces of samples sintered at 500 and 600 °C are smooth, similar to β-NiOOH@β-CoOOH precursor. However, the surface images of samples sintered at 700 and 800 °C are coarse, composing crystal particles between cracks. The EDS (Fig. 8) and SEM of broken samples (Fig. 9) results reveal

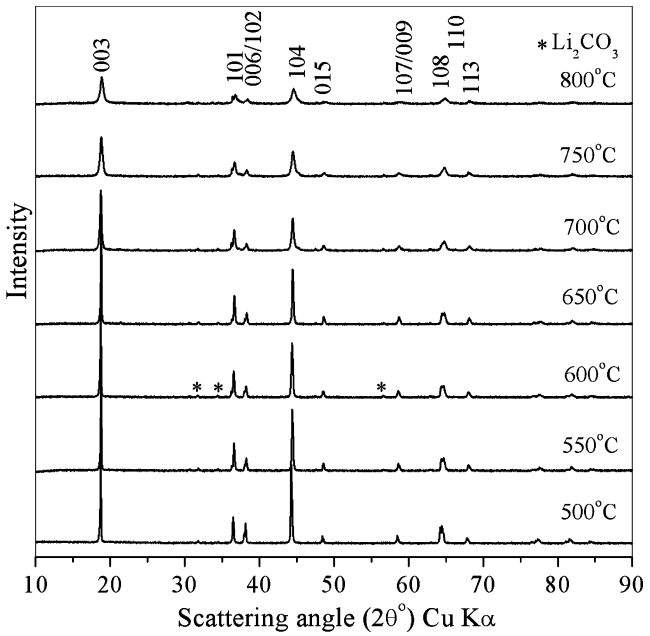

Fig. 5 XRD patterns of resultant samples prepared from β-NiOOH@β-CoOOH and LiOH at different temperatures for 24 h

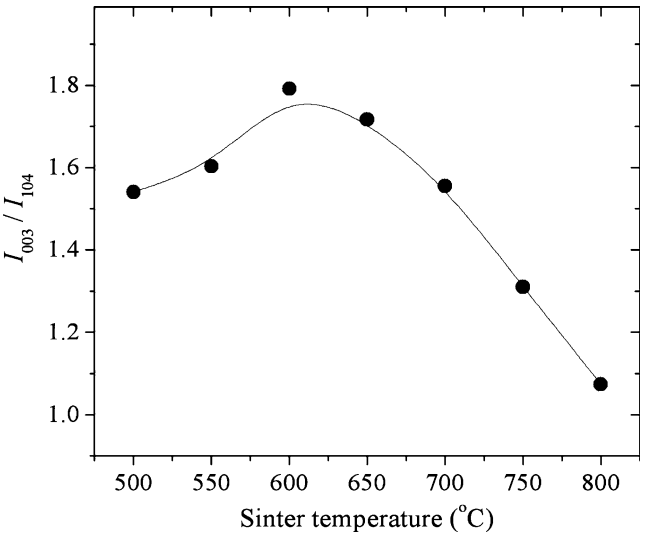

Fig. 6 Intensity ratio of 003 and 104 diffraction peaks of samples prepared from β-NiOOH@β-CoOOH and LiOH at different temperatures for 24 h

that the sample sintered at 600 °C still remain core-shell structure, but the sample sintered at 700 °C has not core-shell structure since the Ni/Co ratio is the same in all the part of spherical particle, and the shell seems to disappear. Ni and Co atoms completely diffused each other, and the absolute Co-doping $LiNi_{1-x}Co_xO_2$ solid solution was formed when the sintered temperature was too high, then, the core-shell structure disappeared [12, 15]. It should be noted that some spheres might crack into small particles during the mechanical mixing of NiOOH@CoOOH and LiOH (Figs. 8 and 9); therefore, the resultant samples might be without integrated core-shell structure.

We also investigated the mixture of β-NiOOH@β-CoOOH and LiOH sintered at 600 °C for different times, and their XRD patterns are shown in Fig. 10. The I_{003}/I_{104} of samples prepared at 12, 24, and 48 h are 1.38, 1.79, and 1.49, respectively. Therefore, the layered property of samples becomes worse if the sintering time is too short or long. The XRD patterns in Fig. 11 also show that the sample prepared from spherical β-NiOOH@β-CoOOH precursor has better layered structured property than that from β-NiOOH or β-$Ni(OH)_2$ precursor at 600 °C for 24 h in the air. However, it is different to XRD pattern of NiOOH@CoOOH precursor, it is difficult to distinguish $LiCoO_2$ or $LiNi_{1-x}Co_xO_2$ diffraction peaks for all the Li-samples. It might be that the intensity of $LiNiO_2$ diffraction peaks is much stronger than those of $LiCoO_2$ or $LiNi_{1-x}Co_xO_2$, then, the diffraction peaks of $LiCoO_2$ or $LiNi_{1-x}Co_xO_2$ were overlaid by $LiNiO_2$.

Figure 12 compares the charge and discharge characteristics of the first cycle of $LiNiO_2$@$LiCoO_2$ and $LiNiO_2$, which are prepared from spherical β-NiOOH@β-CoOOH and β-NiOOH at 600 °C for 24 h, respectively. Though the

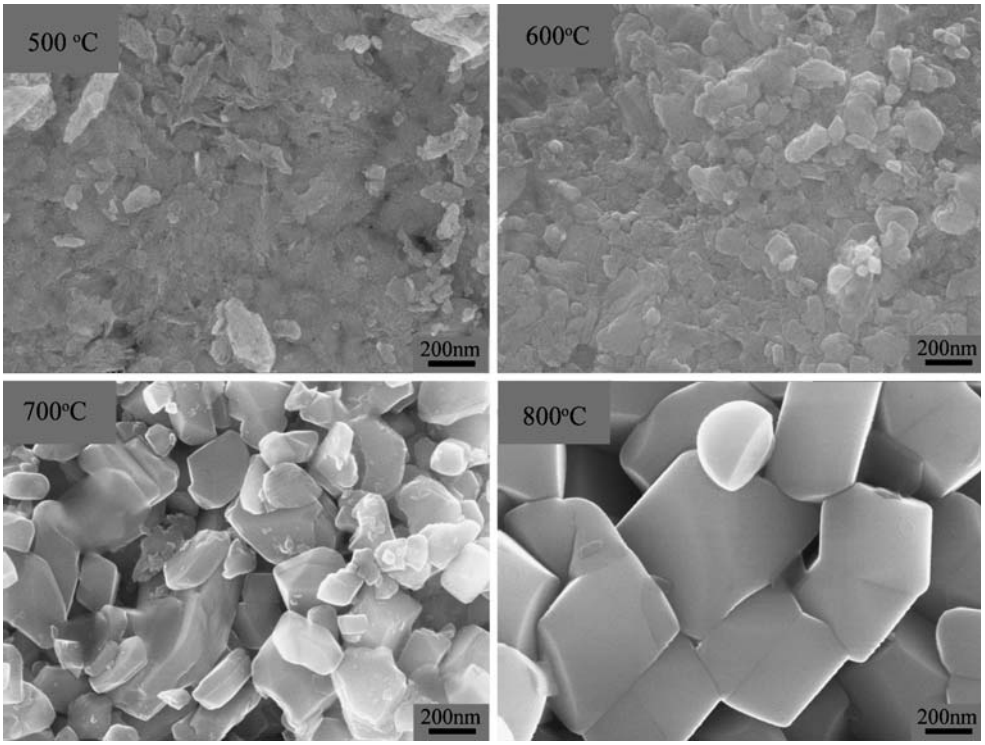

Fig. 7 SEM images of samples prepared from β-NiOOH@β-CoOOH and LiOH at different temperatures for 24 h

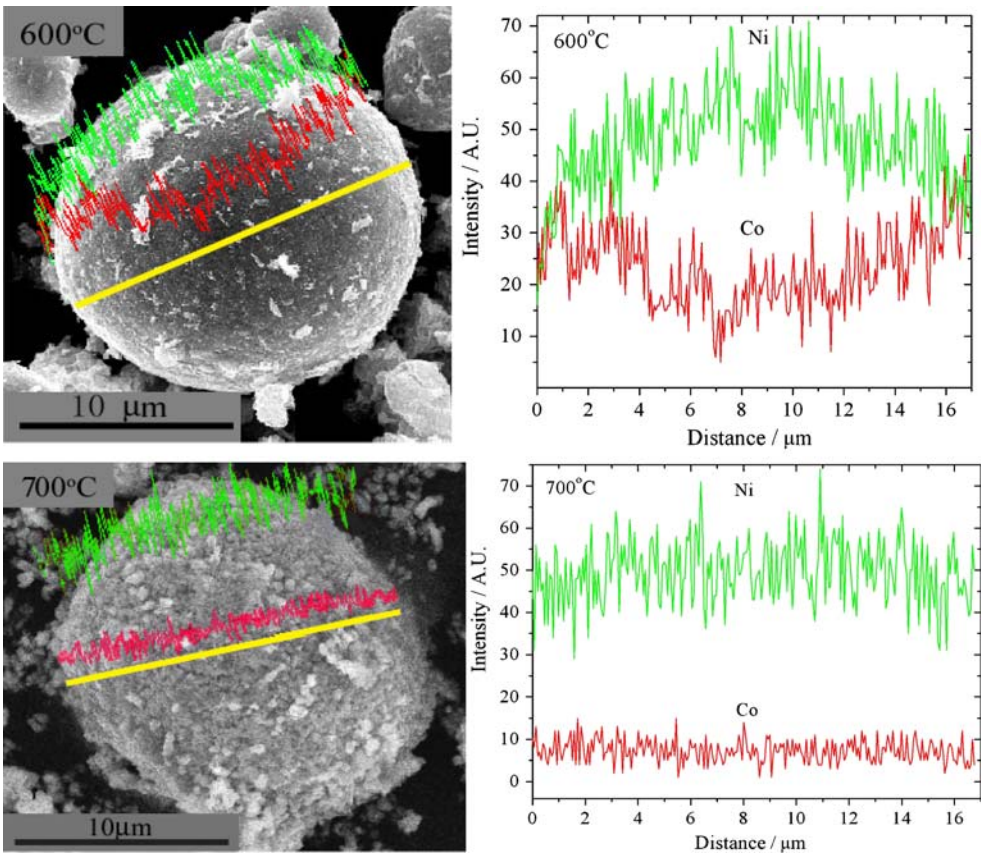

Fig. 8 EDS images of samples prepared from β-NiOOH@β-CoOOH and LiOH at different temperatures for 24 h

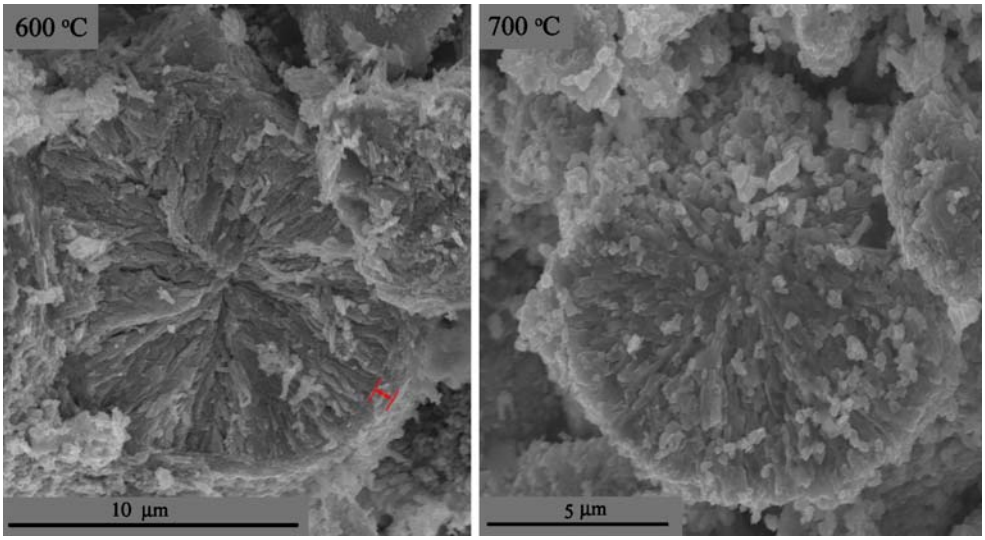

Fig. 9 Cross-sectional SEM images of samples prepared from β-NiOOH@β-CoOOH and LiOH at different temperatures for 24 h

initial specific discharge capacity of $LiNiO_2$@$LiCoO_2$ (181.4 mA h g^{-1}) is slightly lower than that of $LiNiO_2$ (183.9 mA h g^{-1}), the charge–discharge coulombic efficiency of $LiNiO_2$@$LiCoO_2$ (89.4%) is higher than that of $LiNiO_2$ (83.9%). Furthermore, it is obviously observed from Fig. 13 that the $LiNiO_2$@$LiCoO_2$ has better cycleability than $LiNiO_2$. After 20 charge–discharge cycles at current density of 20 mA g^{-1}, the specific discharge capacity retention of $LiNiO_2$@$LiCoO_2$ is 97.4%, markedly higher than 87.7% of $LiNiO_2$. The improvement of cycling performance is attributed to the $LiCoO_2$ shell covered on the surface of $LiNiO_2$, which isolates the $LiNiO_2$'s direct contact from the electrolyte. In addition, Co-modified $LiNiO_2$ can also improve the cycling stability of $LiNiO_2$ [15].

$LiNiO_2$ readily reacts with H_2O and CO_2 in the air atmosphere as the following reactions [18], leading to bad electrochemical performance. It can be clearly concluded from the reactions (1)–(4) that the weight of sample enhances when $LiNiO_2$ reacts with H_2O and CO_2. Therefore, we can easily evaluate the storage stability of $LiNiO_2$-based materials by comparing the weight-enhanced percent of samples at a certain temperature and humidity. It is seen from Fig. 14 that the weight increment of $LiNiO_2$@$LiCoO_2$ is lower than that of $LiNiO_2$ when stored at 30 °C and 65% humidity for 15 days. The spherical $LiNiO_2$@$LiCoO_2$ has better storage stability than $LiNiO_2$ since the stable $LiCoO_2$ outer shell covers the $LiNiO_2$ inter core and insulates its contact with H_2O and CO_2 in the air atmosphere.

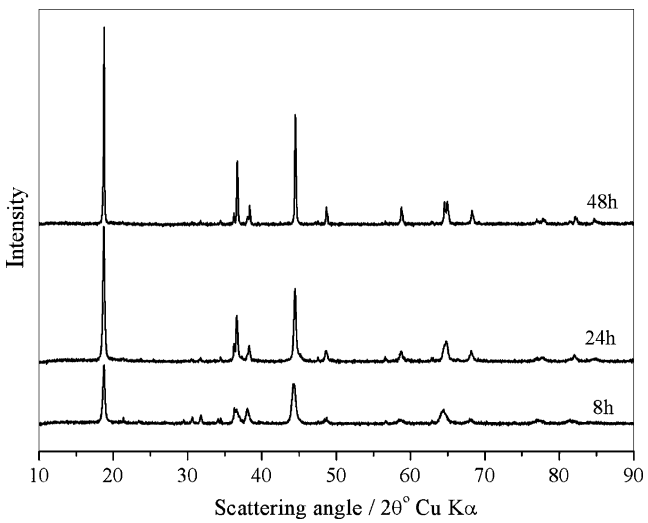

Fig. 10 XRD patterns of resultant samples prepared from β-NiOOH@β-CoOOH and LiOH at 600 °C for different times

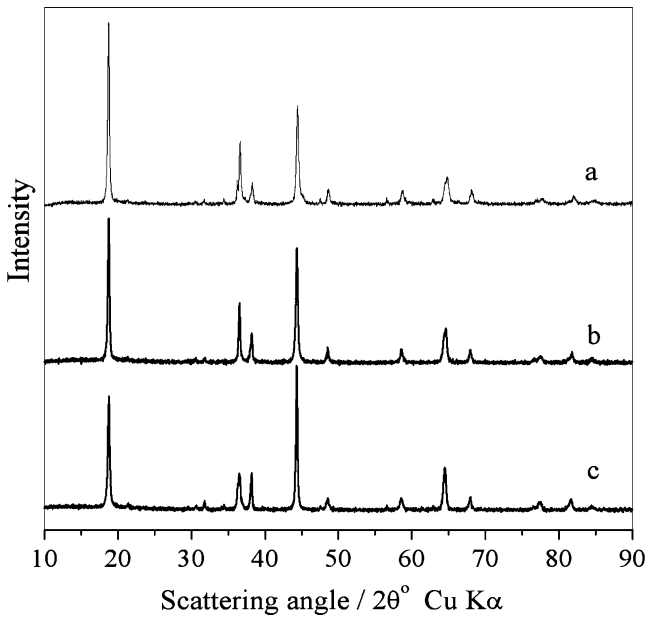

Fig. 11 XRD patterns of resultant samples sintered at 600 °C for 24 h from different precursors and LiOH: *a* β-NiOOH@β-CoOOH; *b* β-NiOOH; *c* β-$Ni(OH)_2$

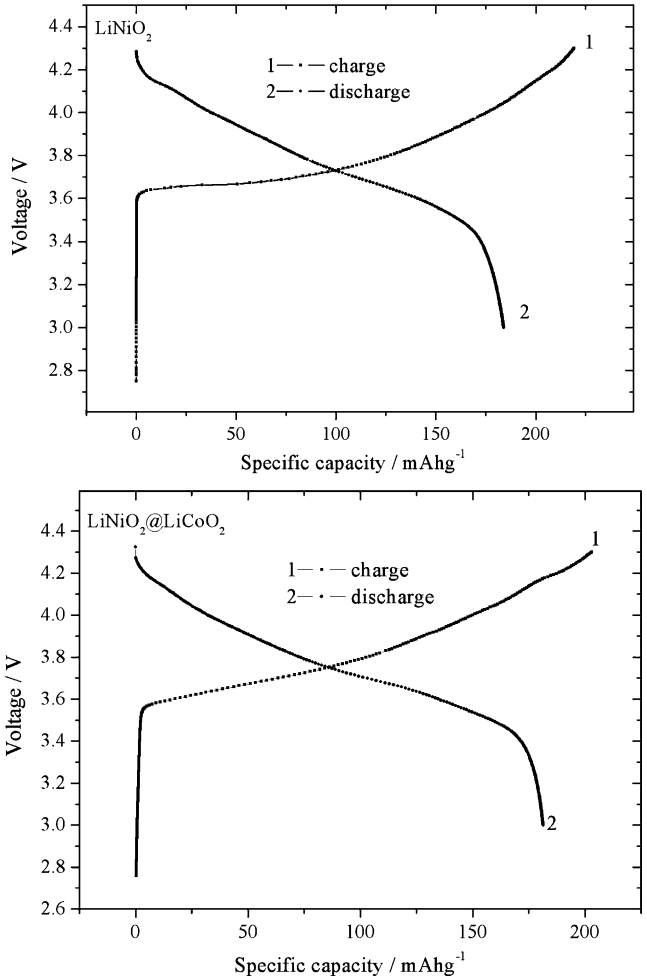

Fig. 12 Charge and discharge curves of $LiNiO_2$@$LiCoO_2$ and $LiNiO_2$

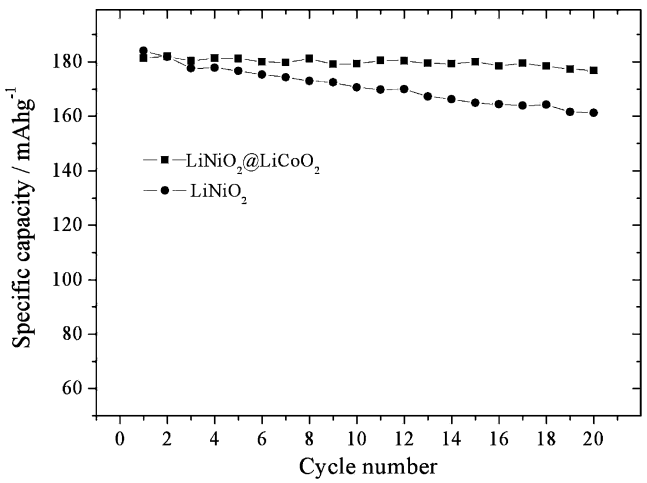

Fig. 13 Cycling performance of $LiNiO_2$@$LiCoO_2$ and $LiNiO_2$ at a constant current of 20 mA g^{-1}

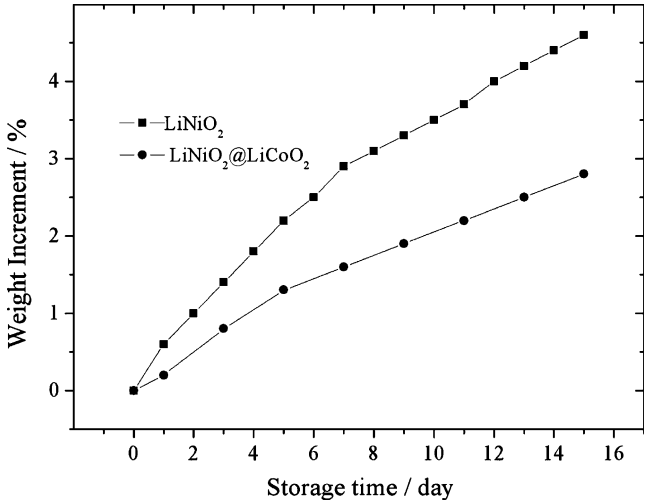

Fig. 14 Weight increment of $LiNiO_2$@$LiCoO_2$ and $LiNiO_2$ stored in 65% humidity at 30 °C

$$LiNiO_2 + x/2H_2O = Li_{1-x}NiO_{2-x/2} + xLiOH \quad (1)$$

$$LiNiO_2 + 1/2H_2O = LiOH + NiO + 1/4O_2 \quad (2)$$

$$LiNiO_2 + y/2CO_2 + y/4O_2 = Li_{1-y}NiO_2 + y/2Li_2CO_3 \quad (3)$$

$$2LiNiO_2 + CO_2 = Li_2CO_3 + 2NiO + 1/2O_2 \quad (4)$$

Conclusions

Spherical $LiNiO_2$@$LiCoO_2$ was synthesized by sintering the mixture of spherical β-NiOOH@β-CoOOH and LiOH in air atmosphere at low temperature. The optimum preparation condition is 600 °C for 24 h in this study. The first discharge capacity of this $LiNiO_2$@$LiCoO_2$ with core-shell structure is 181.4 mA h g^{-1}. The low temperature synthesis of $LiNiO_2$@$LiCoO_2$ also has better cycleability and storage stability than $LiNiO_2$ prepared from spherical β-NiOOH. Spherical $LiNiO_2$@$LiCoO_2$ is a promising cathode material for lithium ion batteries, and the spherical *β-NiOOH@β-CoOOH is an excellent precursor for low temperature synthesis.*

Acknowledgments This work was supported by the National Science Foundation of China (20673089 and 20423002), the Key Scientific Project of Fujian Province of China (2005HZ01-3), and the 973 Program (2009CB939804).

References

1. Sekai K, Azuma H, Omaru A, Fujita S, Imoto H, Endo T, Yamaura K, Nishi Y, Mashiko S, Yokogawa M (1993) J Power Sources 43:241
2. Ma X, Wang C, Cheng J, Sun J (2007) J Solid State Electrochem 11:1139
3. Peres JP, Delmas C, Rougier A, Broussely M, Perton F, Biensan P, Willmann P (1996) J Phys Chem Solids 57:1057
4. Tan KS, Reddy MV, Rao GVS, Chowdari BVR (2005) J Power Sources 141:129
5. Yamada S, Fuliwara M, Kanda M (1995) J Power Sources 54:209
6. Larcher D, Palacin MR, Amatucci GG, Tarascon JM (1997) J Electrochem Soc 144:408
7. Fujita Y, Amine K, Maruta J, Yasuda H (1997) J Power Sources 68:126
8. Sun YZ, Wan PY, Pan JQ, Xu CC, Liu XG (2006) Solid State Ionics 177:1173
9. Gover RKB, Kanno R, Mitchell BJ, Yonemura M, Kawamoto Y (2000) J Eletrochem Soc 147:4045
10. Sivaprakash S, Majumder SB, Nieto S, Katiyar RS (2007) J Power Sources 170:433
11. Dahbi M, Saadoune I, Amarilla JM (2008) Electrochim Acta 53:5266
12. Sun YK, Myung ST, Kim MH, Prakash J, Amine K (2005) J Am Chem Soc 127:13411
13. Sun YK, Myung ST, Park BC, Amine K (2006) Chem Mater 18:5159
14. Sun YK, Myung ST, Parka BC, Prakash J, Belharouak I, Amine K (2009) Nature Materials 8:320
15. Zhong SW, Zhao YJ, Lian F, Li Y, Hu Y, Li PZ, Mei J, Liu QG (2006) Trans Nonferrous Met Soc China 16:137
16. Fu XZ, Xu QC, Hu RZ, Pang PX, Lin JD, Liao DW (2007) J Power Sources 164:916
17. Dahn JR, Sacken UV, Michal CA (1990) Solid State Ionics 44:87
18. Matsumoto K, Kuzuo R, Takeya K, Yamanaka A (1999) J Power Sources 81–82:558